Applied Catalysis B: Environmental 189 (2016) 172–180

Contents lists available at ScienceDirect

Applied Catalysis B: Environmental

journal homepage: www.elsevier.com/locate/apcatb

Electrocatalytic reduction of carbon dioxide on indium coated gas diffusion electrodes—Comparison with indium foil

Ziad Bitar[a,b], Antoine Fecant[a], Emmanuelle Trela-Baudot[a], Sylvie Chardon-Noblat[b], David Pasquier[a,*]

[a] IFP Énergies nouvelles, Rond-point de l'échangeur de Solaize, BP3, 69360 Solaize, France
[b] Université Grenoble Alpes/CNRS, Département de Chimie Moléculaire, UMR 5250, Laboratoire de Chimie Inorganique Redox, BP53, 38041 Grenoble Cedex 9, France

ARTICLE INFO

Article history:
Received 19 November 2015
Received in revised form 29 January 2016
Accepted 16 February 2016
Available online 19 February 2016

Keywords:
Carbon dioxide
Electrocatalysis
Gas diffusion electrode
Formic acid
Indium

ABSTRACT

The electrocatalytic reduction of carbon dioxide to formic acid on metallic electrodes is known to suffer from low current density and rapid surface contamination by electrolyte impurities. Gas diffusion electrodes (GDE) can overcome these problems due to their high specific surface area. In this work, we show a simple method to prepare indium coated gas diffusion electrodes (GDE-In/C) and their physical and electrochemical characterization. Indium is chosen for its ability to reduce CO_2 to formic acid at relatively low overpotential compared to other metals. The catalytic performance of the GDE-In/C is compared to an indium foil using identical operating conditions. During electrolysis in homogeneous aqueous media (dissolved CO_2) at −1.65 V vs. Ag/AgCl, the partial current density toward HCOOH on the GDE-In/C is 7 times higher than on the indium foil with a faradaic efficiency of 45%. The production of formic acid increases by 15% when a continuous flux of CO_2 gas is applied through the GDE-In/C. In addition, the GDE-In/C shows a good resistance to electrolyte impurities and allows to achieve higher current densities. These promising results are a key milestone in the development of a zero gap cell for gas phase CO_2 electroreduction

1. Introduction

One of this century's major challenges is undoubtedly the reduction of atmospheric emissions of carbon dioxide (CO_2). To this end, over recent decades, CO_2 capture and storage (CCS) technologies have been receiving increased attention by research teams around the world, and recently the first industrial scale demonstration CCS plants have been commissioned [1,2]. The high abundance of CO_2 makes it worth considering as a carbon resource; thus, methods for converting it into a product with higher added value are desirable.

Electrochemical reduction seems to be, among many other methods, a promising approach to convert CO_2 into valuable fuels and chemicals. However, one of this technique's grand challenges reported by the Department of Energy (DOE) was the discovery and development of efficient catalysts for CO_2 electroreduction [3]. Depending on the catalyst selectivity and the applied potential, CO_2 is likely to react, in aqueous medium, with water and two electrons resulting in the formation of carbon monoxide (CO) or formic acid (HCOOH) [4]. When a copper (Cu) or copper oxide electrode is used, alcohols and hydrocarbons could be obtained [5,6], but the reaction selectivity is poor and requires more energy [7]. Metals such as Au, Ag, Pd, Co and Zn show high selectivity for reducing CO_2 to CO [8–10]. Metals with high hydrogen evolution overpotential, such as Pb, In, Cd, Tl, Bi and Sn, were shown to efficiently reduce CO_2 into formic acid [11,12]. A high selectivity is achieved when pH is neutral or slightly basic resulting in formate anions instead of formic acid. On Sn and In electrodes, the reduction of CO_2 into formate requires lower over-potential than other metals (Pb, Cd, Bi and Tl). At the same applied current density (5 mA cm^{-2}) in a CO_2 saturated 0.1 M $KHCO_3$ electrolyte, the current efficiency for $HCOO^-$ formation is 94.9% for In and 88.4% for Sn [13].

Formic acid is considered as a convenient and safe liquid compound for hydrogen-storage. It could be either selectively dissociated into hydrogen and CO_2 with the appropriate catalyst [14,15], or used in a Direct Formic Acid Fuel Cell (DFAFC) to recover energy in an electrical form [16].

However, the electrocatalytic reduction of CO_2 in aqueous media at bulk metal electrodes suffers from several drawbacks. Due to the low solubility of CO_2 in water under ambient conditions, the reaction rates and current densities are limited by mass transfer

* Corresponding author.
E-mail address: david.pasquier@ifpen.fr (D. Pasquier).

http://dx.doi.org/10.1016/j.apcatb.2016.02.041
0926-3373/

on solid electrodes. In addition, the low specific surface area of these electrodes and their deactivation due to surface poisoning are among the major factors limiting their utilization in an electrochemical process. Several works have proven that the low reaction rate can be enhanced by elevation of the pressure of CO_2 [17–20]. Another effective way to enhance the reaction rate is the use of Gas Diffusion Electrodes (GDE), which were initially developed for fuel cell technology. Many studies show that the application of GDE for the electrochemical reduction of CO_2 enhances the rate of the process due to their high porosity and high specific surface area [21,22]. Several works mentioned the use of Pb and Sn as catalysts on GDE for $HCOO^-$ formation [23–26]. This work aims at investigating the preparation and study of indium coated gas diffusion electrodes (GDE-In/C) for the electro-reduction of carbon dioxide and evaluating their performance in aqueous electrolytes compared to In foil in identical conditions. To our knowledge very few studies have reported a rigorous comparison of the performance between these two types of electrodes (GDE vs. flat electrode) using the same metal catalyst and identical experimental conditions [27].

This preliminary study refers only to the use and characterization of these electrodes in aqueous media. The results of this work will be used to inform the development of a reactor for gas phase CO_2 reduction, enabling higher reactant concentrations and thus higher current densities.

2. Experimental

2.1. Preparation of In/C catalyst

VULCAN® XC72R carbon (Cabot Corp.) was used as catalyst support (internal pore volume of 2.5 mL g^{-1}). The active phase precursor was $In(NO_3)_3$ hydrate, purchased from Aldrich and used as received. Vulcan carbon was dried at 120 °C until constant mass prior to use. An aqueous solution of indium nitrate 0.23 M (3.1% wt of In) was prepared and used to impregnate the carbon powder. Isometric impregnation method was used to prepare carbon supported indium catalyst (In/C) as follows. 24.2 g of the prepared solution was added dropwise to 9 g of carbon under slow stirring. The resulting mixture was dried at 120 °C for 12 h to remove residual water. This procedure was repeated twice to reach a loading of 20% wt In/C. Then the resulting powder was ground into fine powder. The elimination of nitrate was conducted in a tubular furnace under hydrogen flow of 10 NL h^{-1} at atmospheric pressure. A 2 °C min^{-1} temperature ramp was programmed to reach 400 °C followed by a 2 h plateau. Next, the powder was gradually cooled under argon at the same temperature ramp before exposure to air to prevent pyrophoric reactions. The resulting catalytic powder is here referred to as In/C, even if the metal particles are partially or totally oxidized once exposed to air.

2.2. Manufacturing of gas diffusion electrodes (GDE)

GDE usually consist of a gas diffusion layer (GDL) on which a catalytic layer is deposited. The GDL was purchased from PaxiTech (France) and used as received. A catalytic ink was formulated by mixing the prepared In/C catalyst in ethanol with a 10% Nafion® aqueous solution (PaxiTech). A weight ratio Nafion®/Carbon of 0.9 was used for ink formulation. The ink deposition on the GDL was performed by PaxiTech using an ultrasonic atomizing nozzle system allowing a homogeneous distribution of the catalyst. The In loading in the gas diffusion electrodes was fixed to 1 ± 0.05 mg cm^{-2}. The resulting GDE is referred to as GDE-In/C.

2.3. Catalyst characterizations and products analysis

Scanning electron microscopy (SEM), combined with Energy Dispersive X-ray analysis (EDX) were performed using SUPRA 40 and JEM 2100F microscopes. Powder X-ray diffraction patterns were acquired using a PAN X'pert PRO MPD θ–θ instrument with Bragg-Brentano geometry, equipped with a copper anode (1.54 Å), a proportional counter and variable aperture slots vs. 2θ. The analysis range was from 2 h = 2θ to 72θ, with a step of 0.05 and a counting time of 10 s per step. The specific surface area of the In/C catalyst and the GDE-In/C were calculated by the BET method (ASAP 2420, ASTM D3663-03).

During the electrolysis, gaseous products were sampled from the atmosphere of the electrochemical cell. Gases (CO and H_2) were analyzed on a PerkinElmer Clarus 500 gas chromatograph equipped with a 30 m Carboxen-1010 PLOT capillary GC column (Supelco) and a PDID detector. Helium was used as the carrier gas and quantification of products was insured by using an internal standard (5% methane in CO_2, Air Liquide).

Formic acid was analyzed using a high performance liquid chromatograph (HPLC) equipped with a Polypore Column Type H (4.6×220 mm) coupled with UV detection at 230 nm. The mobile phase was a 10^{-2} M H_2SO_4 aqueous solution at a 0.3 mL min^{-1} flow rate. External standards were used for quantitative HPLC analysis. Each sample is injected three times and the error on the measured concentration was below 1%. Please note that in the pH range of the experiments, the reduction of CO_2 gives mainly formate and not formic acid since the formic acid pK_a is 3.75. Additionally, as expected in a protic electrolyte no oxalate was detected.

2.4. Electrochemical measurements

The catalytic powder was electrochemically characterized using cyclic voltammetry technique. Cyclic voltammogramms were recorded at room temperature, under argon or CO_2 in a three-electrode cell, using an EG & G Princeton Applied Research Model 173 potentiostat/galvanostat equipped with a digital coulometer and a Sefram TGM 164 X-Y recorder. An aqueous solution of 0.1 M Na_2SO_4 was used as electrolyte. Potentials were referred to Ag/AgCl in 3 M KCl reference electrode connected to the working solution by a Luggin capillary. The counter electrode was a Pt foil connected to the solution by a bridge containing the electrolyte. The working electrode was a Pt cavity microelectrode (CμE) [28,29] (~50 μm diameter and 20 μm depth), which was filled with the catalytic powder using the electrode as a pestle. The potential scan rate was 100 mV s^{-1}. For comparative measurements, the working electrode was changed to an indium foil purchased from Alfa Aesar (Puratronic®, 99.9975%) rinsed with ethanol and water before use.

Electrocatalysis experiments were carried out at different applied potentials in the electrochemical H-type cell shown in Fig. 1a. The anodic and cathodic compartments were separated by a Nafion® 117 membrane (Dupont). An aqueous solution of 0.1 M Na_2SO_4 was used as electrolyte (the volume of both anolyte and catholyte was 130 mL). The self-made GDE was used as working electrode and mounted in a polyetheretherketone (PEEK) holder. The geometric surface area of all working electrodes used was 0.95 cm^2. The same reference electrode as above was placed facing the working electrode. The counter electrode was a carbon nanofoam (Marketech International) mounted on a PEEK holder. It is well recognized that carbon is not the best catalyst for oxygen evolution (carbon can also be oxidized). In future studies, we plan to use iridium black coating on the membrane as anode, this catalyst having a significantly lower overpotential for oxygen evolution. Nevertheless, the point we address in this study is focused on the cathode by a relative performance comparison. For some experiments as described in the results, the electrolyte was purified by

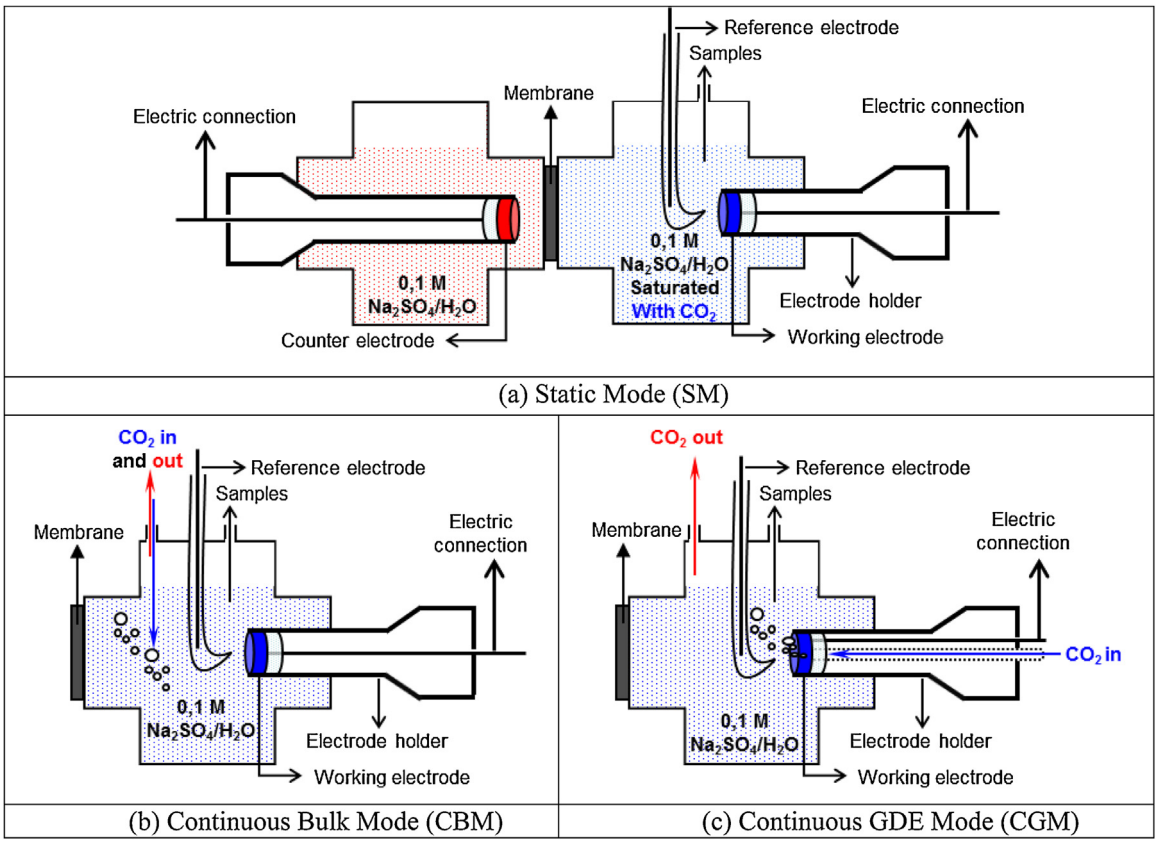

Fig. 1. Schematic representation of the electrochemical H type cell in Static Mode (SM) (a), the cathodic compartment in Continuous Bulk Mode (b), and the cathodic compartment in Continuous GDE Mode (c).

pre-electrolysis on Pt foil at −1.8 V for 1 h. Three modes of electrocatalysis were tested at room temperature in an aqueous solution of 0.1 M Na_2SO_4 (Sigma Aldrich, Ref. 238597). In the first mode, the solution was bubbled with CO_2 until the electrolyte was saturated, then the bubbling was stopped before starting the electrocatalysis and the system is referred as "Static Mode" (SM; Fig. 1a). In the second and third modes, the anodic compartment was not modified, but the cathodic compartment was fed continuously with CO_2 during the electrocatalysis at a flow of 10 mL min^{-1}. When the bubbling is in the bulk of the solution, the system is referred as "Continuous Bulk Mode" (CBM; Fig. 1b) and when it is through the GDE the system is referred as "Continuous GDE Mode" (CGM; Fig. 1c). In contrast with the "static mode" it was not possible to quantify the gaseous products in "continuous modes" where their concentrations were too diluted by the continuous flow of CO_2 to be able to ascertain the analysis.

3. Results and discussion

3.1. Physical characterization of In/C and GDE-In/C

3.1.1. SEM and EDX

The morphology and dispersion of In particles inside In/C and GDE-In/C were characterized by SEM (Fig. 2). Images obtained with In/C catalytic powder reveal the presence of aggregates with different size and shape. Spherical particles of In are detected with sizes from 100 nm to 300 nm (Fig. 2a) and other bulky particles composed of intergrown crystallites reaching a size of few hundreds nm (Fig. 2b). Concerning the GDE-In/C, spherical In particles are clearly visible (Fig. 2c) and of similar size than those of the In/C catalyst. The ink formulation and the deposition process have no visible impact on the catalyst morphology. On a macroscopic view, multiple cracks are shown on the surface (Fig. 2d) probably due to the drying procedure of the GDE. This is related to the high thickness of the deposited layer (70 μm) in order to achieve a loading of 1.06 mg of metal per cm^2 of GDE.

However, EDX mapping reveals a homogeneous distribution of C, In, F and S within the catalytic layer as illustrated in Fig. 3. Since these GDE are designed to be used ultimately in a gas phase environment (zero gap cell), these results are interesting as they are consistent with a high probability of presence of triple phase boundaries. The detection of F and S indicates the presence of the solid polymer electrolyte (Nafion®) insuring a good proton percolation.

Despite the presence of some larger aggregates exceeding 10 μm, the EDX demonstrates that In distribution within the carbon shows some homogeneity. It is presumed that, due to the low melting point of Indium (429.7 K), metal particles could be melted together to form larger particles during the preparation of the catalyst where the temperature reached 673 K.

3.1.2. XRD

Fig. 4 shows the XRD patterns of the carbon support and the prepared In/C catalyst. The broad peak at $2\theta \approx 25^\circ$ on the carrier is due to the C (0 0 2) lattice plane [30,31]. The diffraction peaks of In/C are typical cubic crystalline phase In_2O_3. A minor quantity of tetragonal crystalline phase of In is detected. According to the Scherrer equation, and based on the following lattice plane (2 2 2), (4 0 0), (4 4 0) and (6 2 2) at 2θ equal 30.5, 35.37, 50.91 and 60.53 respectively, In_2O_3 crystallites size was calculated at around 22 nm. Based on the response factors of each phase in our database, we estimate the proportion of In_2O_3/In as 93/7.

The XRD pattern of the GDE-In/C shows the same diffraction peaks of cubic crystalline phase In_2O_3 (data not shown here) and

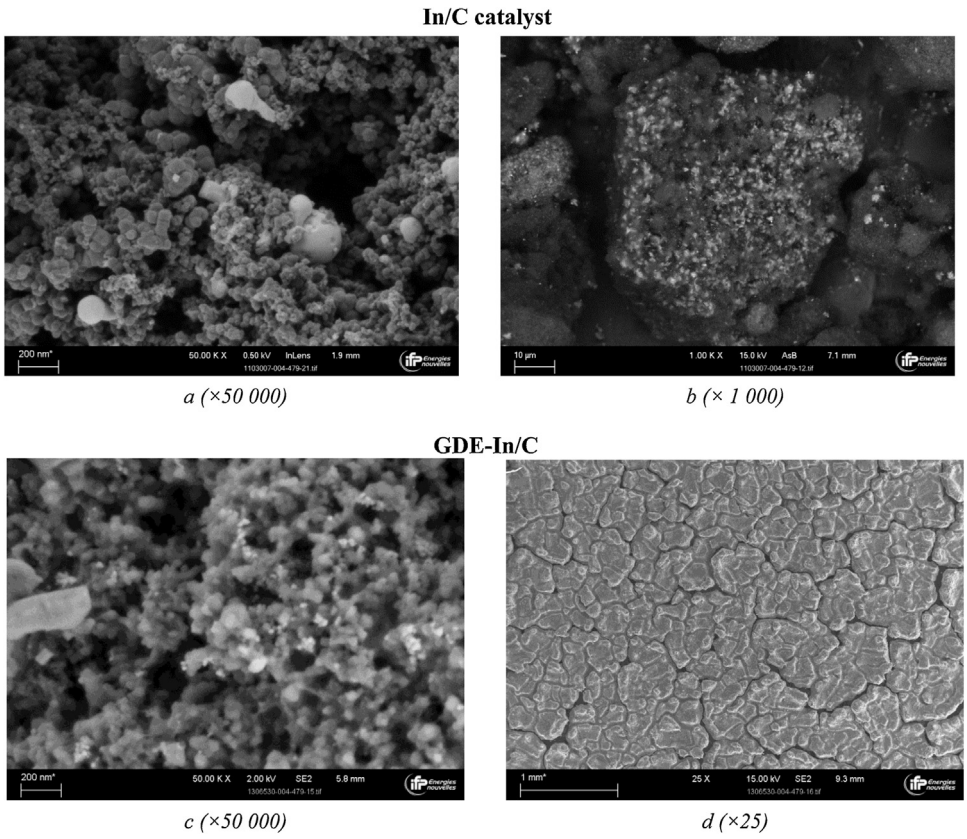

Fig. 2. SEM images with different magnification of In/C catalyst (a), (b) and of corresponding GDE-In/C (c), (d).

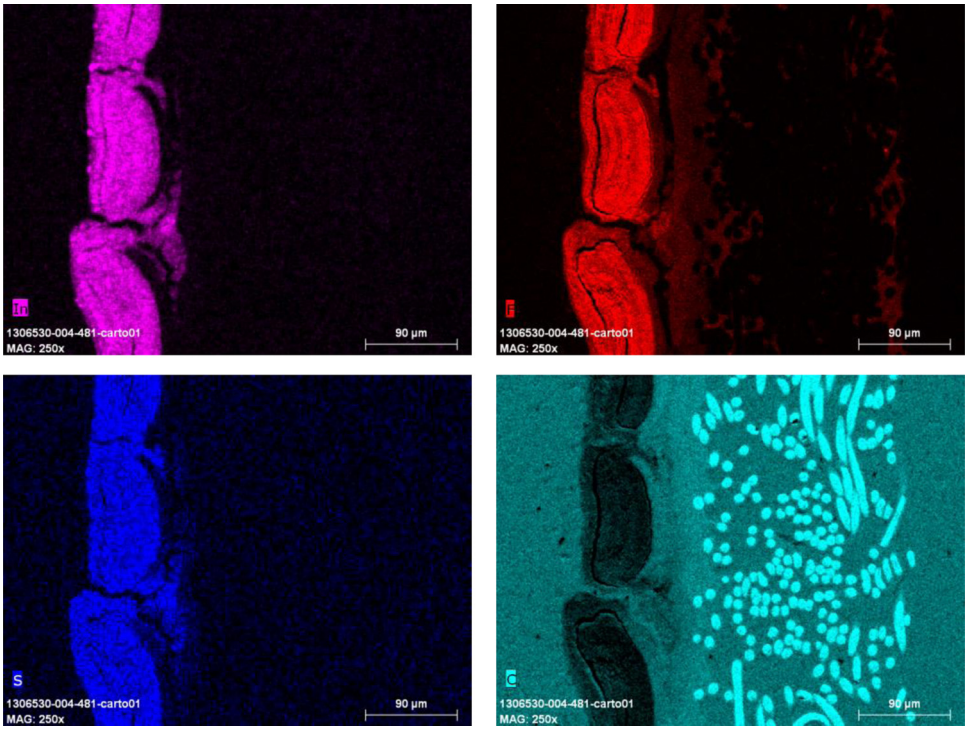

Fig. 3. SEM images of a polished section of GDE-In/C with energy dispersive X-ray (EDX) analysis mapping (In, F, S, C).

the typical peak of the carbon support. However, a hydroxide indium structure ($In(OH)_3$) appears on the GDE-In/C which was absent in the In/C. According to the Scherrer Equation and based on the same lattice plane as above, In_2O_3 crystallites remain around 22 nm and the size of $In(OH)_3$ crystallites is about 40 nm. We suppose that the ink formulation (addition of ethanol and Nafion® solution) has altered the nature of the catalyst by oxidizing the metal or hydrating the metal oxide into $In(OH)_3$. Based on the

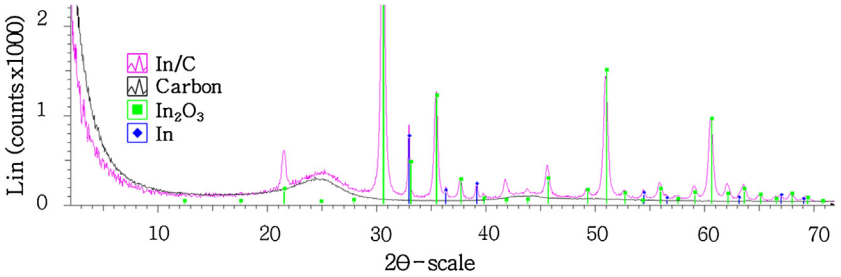

Fig. 4. XRD patterns of the VULCAN® XC72R carbon support (black) and In/C (colored).

response factors of each phase in our database the estimated ratio of In_2O_3/In/$In(OH)_3$ is 78/2/20 respectively.

3.1.3. BET measurements

According to BET measurement, the specific surface area of the carbon powder XC-72R before impregnation was measured at 246 $m^2\ g^{-1}$ which is in agreement with the literature [32], while that of In/C catalyst powder was around 168 $m^2\ g^{-1}$.

BET surface area of the GDL was measured to be 9 $m^2\ g^{-1}$. After deposition, the measured BET surface of GDE-In/C was 16 $m^2\ g^{-1}$. The specific surface area of the active layer of the GDE-In/C has been roughly estimated by using BET measurement. Knowing the geometric surface density of the GDL (133 g m^{-2}), the In/C catalyst density (20% wt) and Nafion®/Carbon weight ratio (0.9), we roughly estimated BET of In/C active layer after deposition is 26 $m^2\ g^{-1}$ by subtracting the GDL contribution (mass and BET surface). If we also subtract the mass of Nafion and thus refer only to the In/C catalyst deposed the estimated BET surface area is around 45 $m^2\ g^{-1}$.

This loss in BET surface area is undoubtedly due to the presence of Nafion® in the formulated ink used to form these GDE. In any case, one should not confuse the BET surface area of the GDE with the real electrochemical surface area which is related to the accessible metal surface in aqueous electrolyte and to the triple phase boundaries in a porous electrode in the gas phase.

3.2. Electrochemical characterization of In/C

In order to measure the redox potentials of In within the powder catalyst (In/C), a Pt cavity microelectrode was employed. This type of electrode allows the electrochemical properties of powder materials to be determined [33]. On the other hand, an In foil was used as a comparison. The cyclic voltammograms of In foil (Fig. 5a) and In/C powder (Fig. 5b) are shown under both argon (plain line) and saturated CO_2 atmospheres (dot lines). Please note that in Fig. 5b, the current is plotted instead of the current density as neither the volume nor the mass of the In/C powder inserted inside the cavity micro-electrode could be known exactly.

On In foil, a large reductive current appears at −1.70 V under argon and reaches a current density of 8.5 mA cm^{-2} at −2.00 V. This current is assigned to water reduction producing H_2. The reverse sweep results in one anodic peak at −0.92 V and represents the formation of a passive film of indium oxide, followed by a steady current indicating thickening of the oxide film. The abrupt current increase at −0.54 V is attributed to the breaking of the oxide film by the oxidation of electrode interface indium layer as reported by Omanovic and Metikoš-Hukovic [34]. The reverse sweep shows a peak at −1.15 V corresponding to the reduction of the indium oxide (or hydroxide) previously formed under anodic current scan.

When the electrolyte is saturated with CO_2, the pH of the 0.1 M Na_2SO_4 solution shifts from 6.4 (under argon) to 4.2. The large reduction current onsets at a less negative potential, attaining a current density of 8.5 mA cm^{-2} at −1.70 V. This high current density at a lower cathodic potential is assigned to both CO_2 and proton reduction, the latter being enhanced due to the pH decrease. The In/In_2O_3 redox potential is also correlated to the pH following the Nernst equation as an acid-base equilibrium occurs.

Inside the In/C powder catalyst, indium species are mainly indium oxide (In_2O_3), as shown in the DRX characterization (Fig. 4). In the cavity microelectrode and under argon (Fig. 5b), a catalytic reductive current reaches 0.42 μA at −1.4 V. This can be attributed to H_2/H_2O redox couple (as for the In foil) and to In_2O_3/In reduction. The reverse sweep shows an anodic peak at −0.94 V indicating the oxidation of the latter electrogenerated In leading to a passive film similar to that shown above for In foil. The second scan allows to observe a cathodic peak at −1.11 V corresponding to the reduction of this In oxide. This peak does not appear in the first scan probably due to the passive behavior of the initial indium oxide.

When saturated with CO_2 the same phenomena appear with a shift of about +200 mV and the current reached 0.42 μA at −1.2 V. This current can be assigned to both CO_2 and proton reduction.

The above study shows a similarity between indium foil and dispersed indium particles inside the In/C catalyst redox behaviors. It also allows identifying the redox couple (indium/indium oxide) for both materials and the possibility to reduce In_2O_3 to In inside In/C when a cathodic potential is applied.

The cyclic voltammetry technique does not reveal the catalytic activation of CO_2-reduction due to the current overlapping with that of water reduction. Furthermore, experiments using the cavity microelectrode were hampered by expulsion of the sample from the cavity due to H_2 bubbling. Therefore chronoamperometric electrolysis, at different applied potentials, have been conducted using the GDE-In/C in order to determine and quantify the products of CO_2 electroreduction in aqueous electrolytes.

3.3. Electrocatalytic performance of the GDE-In/C

3.3.1. Effect of the applied potential

The electrocatalytic reduction of CO_2 was performed at different constant applied potentials in the range from −1.35 V to −1.80 V (vs. Ag/AgCl) at 150 mV intervals. The first experiments were conducted in “Static Mode (SM)” to analyze the products in both gas and liquid phases. During these electrolyses the pH of the electrolytes shifts from 6.8 under Ar to 4.2 under CO_2. It is important to notice we chose to conduct experiments in a non-buffered pH environment, in contrast to what is generally encountered in the literature where hydrogen carbonate electrolytes are commonly used [27,35]. Indeed we aim to be close to the conditions of the zero gap cell we will further use to characterize the gas phase CO_2 electroreduction, where the pH is not controlled. Fig. 6 shows the current efficiency of product formation (CO and $HCOO^-$) vs. the applied potential after 15 h of electrolysis. In the same time the total current density increases as the potential decreases from −1.35 V to −1.80 V (data not shown here). However, the partial current density of $HCOO^-$ and CO reaches a maximum at −1.65 V with a current efficiency of 24% and 6% respectively. Based on these results, the potential −1.65 V was chosen for the experiments described below.

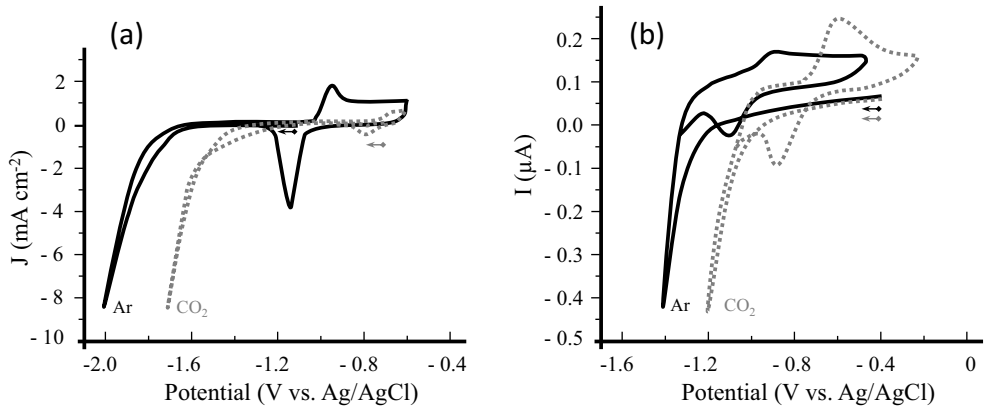

Fig. 5. Cyclic voltammetry for indium foil (a) and In/C catalyst inside the microelectrode (b)—under argon (plain lines) and under CO_2 (dot lines).

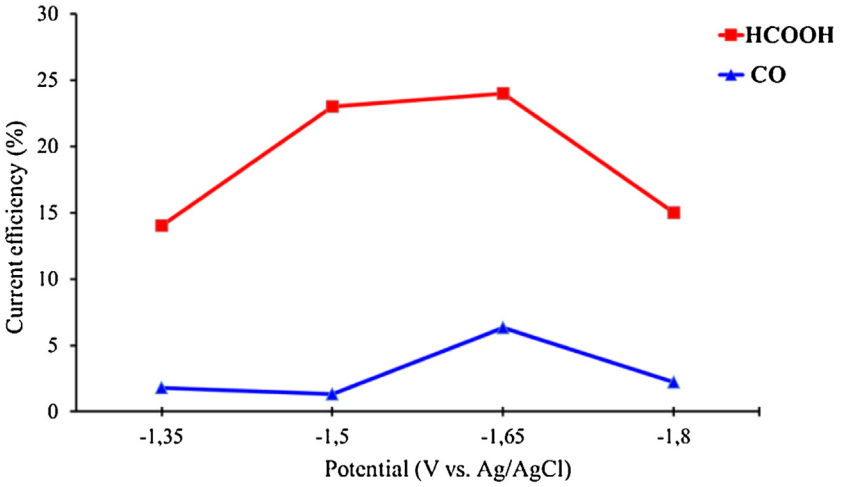

Fig. 6. Effect of the applied potential on the current efficiency of products formed after 15 h using GDE-In/C as working electrode in static mode.

3.3.2. Effect of continuous CO_2 flux

To study the influence of a continuous flux of CO_2 through the catalyst, we studied the performance of GDE-In/C cathodes using the three modes defined in Fig. 1. In the following, all the experimental conditions were identical except for the CO_2 supply. The electrolysis was conducted at −1.65 V in an aqueous solution of 0.1 M Na_2SO_4. The pH variation was tracked during electrocatalysis as a function of the charge passed. As shown in Fig. 7a the pH at t_0 was 4.2 and increased to 5.9 for all modes after 160 C. Fig. 7b plots the accumulated formate concentration vs. charge passed. It is clear that the continuous flux of CO_2 enhances the kinetic rate of formate formation and it is further enhanced when the CO_2 is fed directly through the GDE-In/C. After 160C the formate concentration using the Continuous GDE Mode (CGM) was 15% greater than the Continuous Bulk Mode (CBM) and 45% greater than the Static Mode (SM). A similar behavior using different catalysts on a GDE has already been reported where the CO_2 flux tends to increase the CO_2 conversion [36].

Table 1 shows that the presence of CO_2 at the electrode-electrolyte interface not only improves the kinetics of the reaction but also enhances the catalyst selectivity toward HCOOH formation with a greater current efficiency of 38% at a final pH equal to 5.9. Since the final pH is similar in the three modes, the variations in catalyst selectivity are attributed to the CO_2 feeding condition.

3.3.3. Comparative assessment of GDE In/C vs. indium metal foil

A rigorous comparison between a metallic electrode and a GDE is difficult to obtain by comparing different literature data since many factors can affect the selectivity and the current density of the CO_2 electroreduction, for instance, it is well known that the nature, concentration and pH of the electrolyte can greatly affect the reaction [37]. Another major factor that should be taken into consideration is the design of the electrochemical cell type used (H-type, conventional three-electrode system, batch electrolysis and zero-gap cell ...) which can also affect the faradaic efficiency of the products and current density. For instance, in a conventional undivided three-electrode system, formate can be oxidized at the anode [38] whereas using an H-type cell divided by a membrane (e.g., Nafion® as for this study) its oxidation is prevented by the low crossover of formate anion through the Nafion® [39].

Therefore, we have operated a meaningful comparison between different electrodes under identical conditions and in the same electrochemical cell. The electrocatalytic activities of both GDE-In/C and indium foil were compared at −1.65 V in the Continuous Bulk Mode since the Continuous GDE Mode could not be performed with the indium foil. Table 2 shows the results obtained on both electrodes after 160C. The current efficiency for HCOOH production is three times higher on the GDE-In/C (32%) than on the indium foil (11%). This difference is also notable when comparing the $HCOO^-$ partial current density ($j_{(HCOOH)}$) where the GDE-In/C is seven times more active than the In foil.

The current efficiency of formate production as a function of the charge is shown in Fig. 8a for both electrodes. The selectivity of In foil is higher for the first coulombs (68%) but falls to 35% after 32 C and decreases to 11% after 160 C while the GDE-In/C selectivity tends to stabilize after 60 C to 30%. During electrolysis,

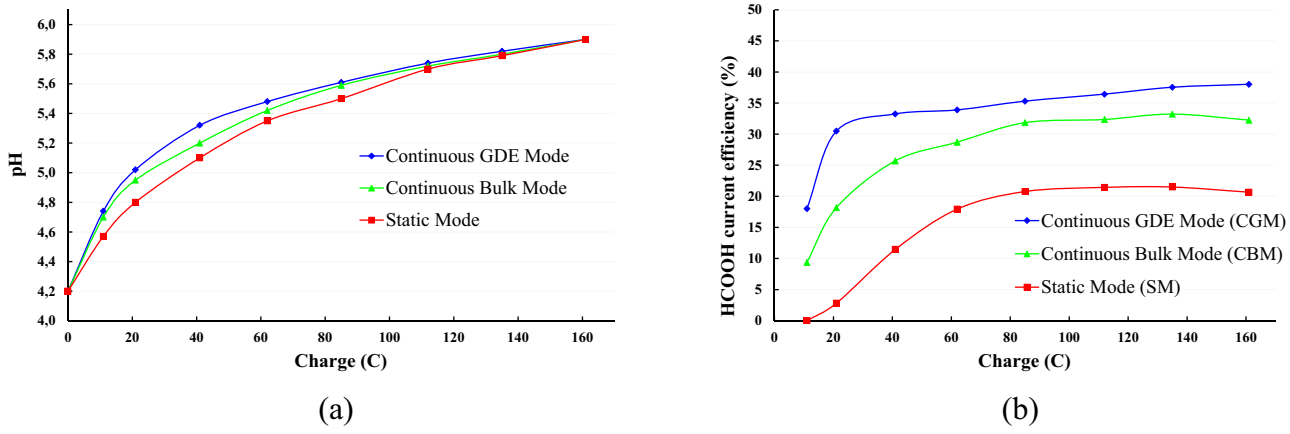

Fig. 7. pH (a) and cumulative $HCOO^-$ concentration (b) plotted against the charge passed on GDE-In/C at −1.65 V in different modes of CO_2 supply.

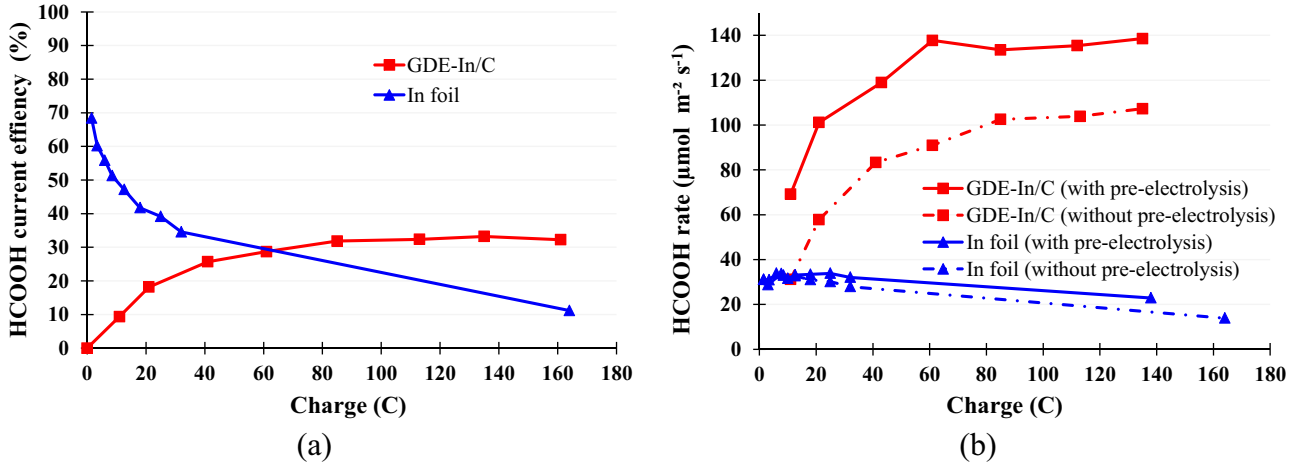

Fig. 8. (a) HCOOH current efficiency plotted against the charge passed on GDE-In/C and In foil at −1.65 V without pre-electrolysis of the electrolyte and (b) HCOOH production rate (normalized by the geometric surface area of the electrode) as a function of the charge passed on GDE-In/C and on In foil with and without pre-electrolysis of the electrolyte.

Table 1
Obtained results on GDE-In/C at −1.65 V using the three different modes after 160 C.

Mode	j (mA cm^{-2})	$j_{(HCOOH)}$ (mA cm^{-2})	HCOOH current efficiency (%)	Time (min)
SM	6.7	1.4	21	420
CBM	6.4	2.1	32	450
CGM	7.5	2.8	38	405

Table 2
Comparison of Indium foil and GDE-In/C at −1.65 V after 160 C in non-purified electrolyte.

Electrode	j (mA cm^{-2})		$j_{(HCOOH)}$ (mA cm^{-2})	HCOOH current efficiency (%)	Time (min)
	After 25 C	After 160 C			
Indium foil	1.9	4.2	0.3	11	1200
GDE-In/C	6.2	6.4	2.1	32	450

Table 3
Comparison of Indium foil and GDE-In/C at −1.65 V after 135 C in purified electrolyte.

Electrode	j (mA cm^{-2})		$j_{(HCOOH)}$ (mA cm^{-2})	HCOOH current efficiency (%)	Time (min)
	After 25 C	After 135 C			
Indium foil	1.9	2.6	0.4	22	1200
GDE-In/C	6.1	6.3	2.8	45	400

we have observed on the In foil electrode a black deposit being formed, which could be responsible for the decrease in selectivity and the increase in current, probably linked to hydrogen evolution.

Further SEM and EDS characterizations of the In foil surface after electrolysis confirmed a poisoning of the electrode surface by dif-

ferent metals such as Zn, Ni, and Fe and also revealed the presence of carbon and oxygen.

Many workers have highlighted the deactivation of metal electrodes during electrolysis but no agreement is found for its reason. Some research groups have attributed it to the deposition of electrolyte impurities [40]. Other researchers reported that the electrode surface may be contaminated with some carbonaceous substance [41,42]. We have purified the electrolyte solution by pre-electrolysis in the same cell used for the electrolysis of CO_2 to avoid contamination during the transfer.

We assume that the GDE-In/C has better performance than the In foil and is less vulnerable to impurities as well. To support this contention the same experiment has been repeated after purifying the electrolyte by pre-electrolysis to remove the impurities. Table 3 indicates the new results obtained on the two different electrodes after 135 C. When the electrolyte is purified prior to CO_2 electrolysis, the HCOOH current efficiency on the In foil is doubled from 11% to 22% for the same electrolysis duration (1200 min). Whereas the relative gain by electrolyte purification with the GDE-In/C (up to 45% current efficiency toward $HCOO^-$) is low. It means the GDE-In/C has a better resistance to contamination. The partial current density to $HCOO^-$ for the GDE-In/C remains seven times higher than on the In foil.

The evolution of the production rate of HCOOH with the charged passed is compared in Fig. 8b for both GDE-In/C and In foil, with or without electrolyte purification. This rate is normalized by the surface area of the electrode and thus expressed in $\mu mol\ m^{-2}\ s^{-1}$. We recall that these electrolyses were made under identical operating conditions by using the same applied potential (−1.65 V) and without pH control (range 4.2–5.9). The electrolyte purification improves the efficiency of both electrodes although it is more pronounced for the GDE. It is noteworthy that the GDE-In/C even in unpurified electrolyte leads to better results than the In foil in a purified electrolyte. The rate of HCOOH formation starts to increase for the GDE-In/C and stabilizes after 60 C passed, whereas for the In foil, this rate is roughly stable and then decreases after 18 C without pre-electrolysis and after 30 C with pre-electrolysis. After electrolysis in a purified electrolyte we observed a very small amount of impurities of similar nature remaining at the surface of the In foil.

4. Conclusion

In this work, indium coated gas diffusion electrodes have been prepared by a simple method using a catalytic powder comprising In particles on a porous carbon support. This catalyst has been formulated into an ink which has been deposited by ultrasonic spraying on a gas diffusion layer.

Physical and electrochemical characterizations of the In/C catalyst and the corresponding prepared GDE-In/C confirmed there was negligible modification of the catalytic active phase during the different preparation steps. However, a decrease in specific surface area of the catalytic layer of the GDE due to the presence of Nafion® was observed.

During electrolysis in homogeneous aqueous media (dissolved CO_2) at −1.65 V vs. Ag/AgCl, a better performance of In gas diffusion electrode compared to In foil has been demonstrated. The partial current density toward HCOOH on the GDE-In/C is 7 times higher than on the indium foil with a faradaic efficiency of 45%. The production of formic acid increases by 15% when a continuous flux of CO_2 gas is applied through the GDE-In/C. These improvements are partly due to the larger surface area of the GDE promoting a better diffusion of reactants and products in comparison with a simple 2D surface of indium foil. However the contribution to the catalytic activity arising from the porous carbon surface is unknown and should be further investigated.

Moreover an increase in selectivity for the GDE compared to In foil was observed, which has been attributed to improved tolerance to impurities in the electrolyte. This is thought to be due to the much higher surface area of the In catalyst, together with the absorption property of the carbon support, meaning a smaller proportion of active catalytic sites are poisoned by impurities. Future studies will take into consideration other parameters such as metal loading in the catalytic layer, the thickness of this layer as well as the nature and concentration of solid polymer electrolyte used as a binder.

These results are a key milestone in the development of a zero gap cell for gas phase CO_2 electroreduction. Such a device would enable significantly higher CO_2 concentration at the cathode, thus lowering the diffusional limitation to allow high current density and, as suggested by this present work, improved selectivity toward formic acid.

Acknowledgements

The authors acknowledge support from LabEx ARCANE (ANR-11-LABX-0003-01). The authors would like to thank the PaxiTech Company for preparing and depositing the catalytic layers and for fruitful discussions. We also wish to thank Dr. Edward Brightman for his thorough proofreading of the manuscript.

References

[1] A. Mathieson, J. Midgley, K. Dodds, I. Wright, P. Ringrose, N. Saoul, Lead. Edge 29 (2010) 216–222.
[2] K. Michael, A. Golab, V. Shulakova, J. Ennis-King, G. Allinson, S. Sharma, T. Aiken, Int. J. Greenh. Gas Control 4 (2010) 659–667.
[3] A.T. Bell, B.C. Gates, D. Ray, M.R. Thompson, Basic Research Needs: Catalysis for Energy, PNNL-17214, Pacific Northwest National Laboratory, Richland, WA, 2008.
[4] M. Jitaru, D.A. Lowy, M. Toma, B.C. Toma, L. Oniciu, J. Appl. Electrochem. 27 (1997) 875–889.
[5] J. Albo, A. Sáez, J. Solla-Gullón, V. Montiel, A. Irabien, Appl. Catal. B: Environ. 176–177 (2015) 709–717.
[6] M. Gattrell, N. Gupta, A. Co, J. Electroanal. Chem. 594 (2006) 1–19.
[7] Y. Hori, R. Takahashi, Y. Yoshinami, A. Murata, J. Phys. Chem. B 101 (1997) 7075–7081.
[8] S. Pérez-Rodríguez, N. Rillo, M.J. Lázaro, E. Pastor, Appl. Catal. B: Environ. 163 (2015) 83–95.
[9] A. Salehi-Khojin, H.-R.M. Jhong, B.A. Rosen, W. Zhu, S. Ma, P.J.A. Kenis, R.I. Masel, J. Phys. Chem. C 117 (2013) 1627–1632.
[10] C. Delacourt, P.L. Ridgway, J.B. Kerr, J. Newman, J. Electrochem. Soc. 155 (2008) B42–B49.
[11] Y. Hori, Modern Aspects of Electrochemistry, Springer, New York, 2008, pp. 89–189.
[12] B. Innocent, D. Pasquier, F. Ropital, F. Hahn, J.M. Leger, K.B. Kokoh, Appl. Catal. B: Environ. 94 (2010) 219–224.
[13] Y. Hori, H. Wakebe, T. Tsukamoto, O. Koga, Electrochim. Acta 39 (1994) 1833–1839.
[14] F. Joo, Chemsuschem 1 (2008) 805–808.
[15] M. Grasemann, G. Laurenczy, Energy Environ. Sci. 5 (2012) 8171–8181.
[16] N.V. Rees, R.G. Compton, J. Solid State Electrochem. 15 (2011) 2095–2100.
[17] Y. Hori, A. Murata, H. Takahashi, S. Suzuki, J. Am. Chem. Soc. 109 (1987) 5023–5025.
[18] G. Kyriacou, A. Anagnostopoulos, J. Electroanal. Chem. 322 (1992) 233–246.
[19] K. Hara, A. Tsuneto, A. Kudo, T. Sakata, J. Electrochem. Soc. 141 (1994) 2097–2103.
[20] M. Todoroki, K. Hara, A. Kudo, T. Sakata, J. Electroanal. Chem. 394 (1995) 199–203.
[21] K. Hara, T. Sakata, J. Electrochem. Soc. 144 (1997) 539–545.
[22] C.M. Sánchez-Sánchez, V. Montiel, D.A. Tryk, A. Aldaz, A. Fujishima, Pure Appl. Chem. 73 (2001) 1917–1927.
[23] G.K.S. Prakash, F.A. Viva, G.A. Olah, J. Power Sources 223 (2013) 68–73.
[24] F. Köleli, T. Atilan, N. Palamut, M. Gizir, R. Aydin, H. Hamann, J. Appl. Electrochem. 33 (2003) 447–450.
[25] R.L. Machunda, J. Lee, J. Lee, Surf. Interface Anal. 42 (2010) 564–567.
[26] R.L. Machunda, H. Ju, J. Lee, Curr. Appl. Phys. 11 (2011) 986–988.
[27] A. Del Castillo, M. Alvarez-Guerra, A. Irabien, AIChE J. 60 (2014) 3557–3564.
[28] V. Vivier, C. Cachet-Vivier, C.S. Cha, J.Y. Nedelec, L.T. Yu, Electrochem. Commun. 2 (2000) 180–185.
[29] C. Cachet-Vivier, V. Vivier, C.S. Cha, J.Y. Nedelec, L.T. Yu, Electrochim. Acta 47 (2001) 181–189.
[30] Y. Wang, T.S. Nguyen, X. Liu, X. Wang, J. Power Sources 195 (2010) 2619–2622.
[31] D. Rathod, M. Vijay, N. Islam, R. Kannan, U. Kharul, S. Kurungot, V. Pillai, J. Appl. Electrochem. 39 (2009) 1097–1103.

[32] J. Qi, Y. Gao, S. Tang, L. Jiang, S. Yan, J. Guo, Q. Xin, G. Sun, Chin. J. Catal. 27 (2006) 708–712.
[33] V. Vivier, C.C. Cachet-Vivier, B.L. Wu, C.S. Cha, J.Y. Nedelec, L.T. Yu, Electrochem. Solid State Lett. 2 (1999) 385–387.
[34] S. Omanovic, M. Metikoš-Hukovic, J. Appl. Electrochem. 27 (1997) 35–41.
[35] Y. Hori, in: C. Vayenas, R. White, M. Gamboa-Aldeco (Eds.), Modern Aspects of Electrochemistry, Springer, New York, 2008, pp. 89–189.
[36] J. Albo, A. Irabien, J. Catal. (2015), http://dx.doi.org/10.1016/j.jcat.2015.11.014.
[37] J. Wu, F. Risalvato, X.-D. Zhou, ECS Trans. 41 (2012) 49–60.
[38] W. Lv, R. Zhang, P. Gao, L. Lei, J. Power Sources 253 (2014) 276–281.
[39] Y.-W. Rhee, S.Y. Ha, R.I. Masel, J. Power Sources 117 (2003) 35–38.
[40] Y. Hori, S. Suzuki, J. Res. Int. Catal. Hokkaido Univ. 30 (1982) 81–88.
[41] D.W. DeWulf, T. Jin, A.J. Bard, J. Electrochem. Soc. 136 (1989) 1686–1691.
[42] S. Wasmus, E. Cattaneo, W. Vielstich, Electrochim. Acta 35 (1990) 771–775.